A Journal of the Gesellschaft Deutscher Chemiker

Angewandte International Edition GDCh Chemie

www.angewandte.org

Accepted Article

Title: N-Heterocyclic Carbene Boranes as Reactive Oxygen Species-Responsive Materials: Application to the Two-Photon Imaging of Hypochlorous Acid in Living Cells and Tissues

Authors: Yen Leng Pak, Sang Jun Park, Di Wu, BoHyun Cheon, Hwan Myung Kim, Jean Bouffard, and Juyoung Yoon

To be cited as: *Angew. Chem. Int. Ed.* 10.1002/anie.201711188
Angew. Chem. 10.1002/ange.201711188

Link to VoR: http://dx.doi.org/10.1002/anie.201711188
http://dx.doi.org/10.1002/ange.201711188

WILEY-VCH

10.1002/anie.201711188

COMMUNICATION

WILEY-VCH

N-Heterocyclic Carbene Boranes as Reactive Oxygen Species-Responsive Materials: Application to the Two-Photon Imaging of Hypochlorous Acid in Living Cells and Tissues

Yen Leng Pak,[†][a] Sang Jun Park,[†][b] Di Wu,[†][a] BoHyun Cheon,[a] Hwan Myung Kim,*[b] Jean Bouffard,*[a] and Juyoung Yoon*[a]

Abstract: N-Heterocyclic carbene (NHC) boranes undergo oxidative hydrolysis to give imidazolium salts with excellent kinetic selectivity for HOCl over other reactive oxygen species (ROS), including peroxides and peroxynitrate. Selectivity for HOCl results from the electrophilic oxidation mechanism of NHC boranes, which stands in contrast to the nucleophilic oxidation mechanism of arylboronic acids with ROS. The change in polarity that accompanies the conversion of NHC boranes to imidazolium salts can control the formation of emissive excimers, forming the basis for the design of the first fluorescence probe for ROS based on the oxidation of B–H bonds. Two-photon microscope (TPM) ratiometric imaging of HOCl in living cells and tissues is demonstrated.

The oxidation of C–B bonds has played a prominent role in the design of materials responsive to ROS. In particular, the borono-Dakin oxidation of arylboronic acids and their esters has been exploited in the development of fluorogenic probes for the detection of hydrogen peroxide (H_2O_2) and endogenous hydroperoxides (ROOH),[1] hypochlorite (OCl^-),[2] or peroxynitrate ($ONOO^-$).[3] Arylboronic acids and their esters are oxidized to phenols with a kinetic selectivity of ca. $10^6 : 10^{3\text{-}4} : 1$ for peroxynitrate, hypochlorite, and peroxide, respectively.[3a] Nevertheless, claims of selectivity for each of these ROS have been reported in solution assays and cell imaging experiments.[4,5] C–B bond oxidation of arylboronates by ROS has also been widely used as a trigger in programmed depolymerization, sensing amplification, drug delivery, and theragnostics.[4b,6]

In view of the need for ROS-responsive materials that are not merely selective but instead specific, it is remarkable that designs relying on the oxidation of B–H bonds have so far been overlooked. Although hydroboranes and borohydrides have been among the most popular and selective reducing agents since the 1950's, their sensitivity to aerobic oxidation or hydrolysis has constrained their applications as ROS-responsive materials. The reactivity of hydroboranes is tamed by the formation of adducts with a Lewis base.[7] In particular, NHC boranes[8] have emerged as attractive reagents that are stable to air, column chromatography, Brønsted acids with a $pK_a > 2$,[9] or even recrystallization from boiling water.[10] Furthermore, Curran, Lacôte and co-workers have demonstrated that NHC boranes can perform as either radical[11] or ionic[9,12] reductants.[8]

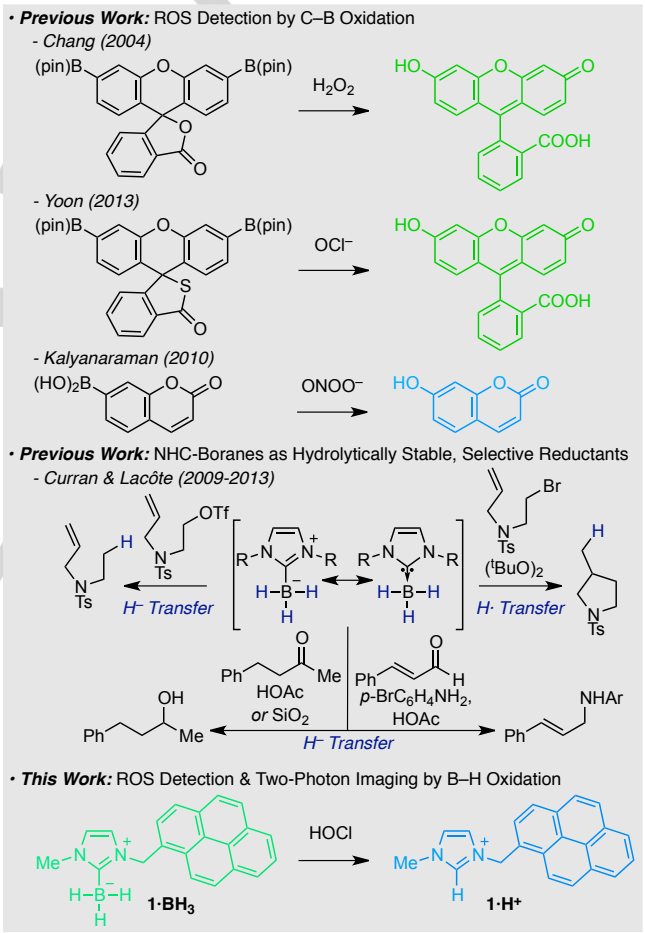

Herein, we report the first fluorescence imaging probe for ROS based on the selective oxidation of a B–H bond. This probe (**1·BH$_3$**) is composed of a NHC borane as the ROS reaction site, and of a pyrene as fluorescence reporter. Because of its low polarity, **1·BH$_3$** reversibly forms colloidal aggregates, facilitating pyrene excimer emission.[13,14] Selective oxidative hydrolysis of the B–H bonds of **1·BH$_3$** by aq. HOCl results in the formation of the imidazolium salt **1·H$^+$**, which exclusively emits as a distinct monomeric species. **1·BH$_3$** enables the ratiometric imaging of biologically relevant HOCl levels in living cells and tissues using TPM.[15]

[a] Y. L. Pak, Dr. D. Wu, B. Cheon, Prof. J. Bouffard, Prof. J. Yoon
Department of Chemistry and Nano Science (BK 21 Plus)
Ewha Womans University, Seoul 03760, Korea
bouffard@ewha.ac.kr, jyoon@ewha.ac.kr
[b] Sang Jun Park, Prof. H. M. Kim
Department of Chemistry and Energy Systems Research
Ajou University, Suwon 443-749, Korea
kimhm@ajou.ac.kr
[†] These authors contributed equally to this work.

Supporting information for this article is given via a link at the end of the document

The absorption and emission spectra of **1·HBr** (10 μM) in phosphate-buffered saline solution (PBS) (10 mM, 99:1 H_2O:CH_3CN, pH 7.4, 25°C) reflect those of an isolated pyrene chromophore. By contrast, chromophore stacking is unmistakable in the emission spectra of **1·BH$_3$**, which features the characteristically broad pyrene excimer band centered near 477 nm (Figure S1). Addition of NaOCl to **1·BH$_3$** results in its immediate conversion to a species indistinguishable from **1·HBr** (Figures 1 and S1). Analysis of the reaction mixture by ESI-MS confirmed the disappearance of **1·BH$_3$**, and its conversion to the imidazolium salt **1·H$^+$** (Figure S2).

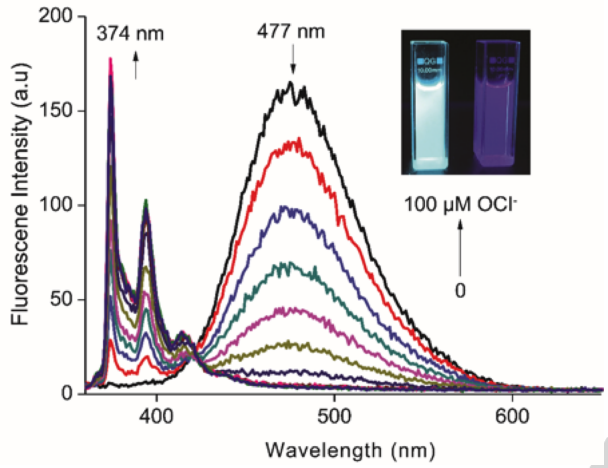

Figure 1. Fluorescence titration of **1·BH$_3$** (10 μM) upon addition of NaOCl (0-100 μM) in PBS (10 mM, pH 7.4) after 1 min at room temperature, with excitation at 350 nm. Inset: Photographs of **1·BH$_3$** before (left) and after (right) the addition 10 equiv. of NaOCl under UV irradiation (365 nm).

The conversion of **1·BH$_3$** to **1·H$^+$** was followed by plotting the ratio of the fluorescence emission intensities in the green (477 nm) and blue (374 nm) color regions (F_{477}/F_{374}), which decreases ca. 540-fold in less than one minute upon the addition of 100 μM NaOCl (Figure S3; $t_{1/2}$ = 1.5 s for [**1·BH$_3$**]·[HOCl/OCl$^-$] = 1x10^{-9} M^2). The detection limit for HOCl/OCl$^-$ in this ratiometric fluorescence assay (3 μM, Figures S4-S5) is far below the physiological concentrations generated by neutrophils (20-400 μM).[16] Probe **1·BH$_3$** is highly selective for HOCl/OCl$^-$ over other ROS and relevant interferences. As shown in Figure 2, only the addition of NaOCl gave rise to a significant change of the F_{477}/F_{374} fluorescence ratio. Other species including hydrogen peroxide, *tert*-butyl hydroperoxide, peroxynitrite, nitric oxide (·NO), hydroxyl (HO·), peroxyl radicals (ROO·), formaldehyde, acetone, or glutathione disulfide (GSSG) only resulted in comparably minor changes in the fluorescence ratio (Figures S6-S11). Furthermore, the stability of the probe **1·BH$_3$**, and the magnitude of the response to HOCl/OCl$^-$ were unchanged in a physiologically relevant range from pH 2 to 10 (Figure S12).

To gain insight into the conversion of **1·BH$_3$** to **1·H$^+$** and its selectivity for HOCl over other ROS, NMR titration experiments were carried out between **2·BH$_3$** and ^{t}BuOCl as surrogates for **1·BH$_3$** and HOCl, respectively (Scheme 1, and Figures S13-S19).

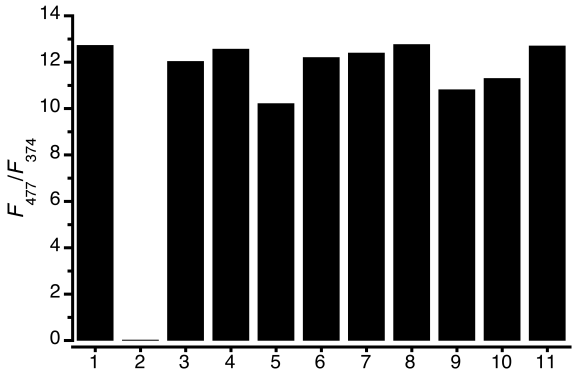

Figure 2. Relative fluorescence responses of **1·BH$_3$** (10 μM) to various ROS and other possible interferences: 1. Blank, 2. NaOCl, 3. H_2O_2, 4. ^{t}BuOOH, 5. ROO•, 6. ONOO$^-$, 7. HO•, 8. •NO, 9. HCHO, 10. Me_2CO, 11. GSSG (10 equiv, 100 μM) in PBS (10 mM, pH 7.4) after 1 min at room temperature.

In dry $CDCl_3$, the oxidation of **2·BH$_3$** to **2·BCl$_3$** is instantaneous (< 30 s), and likely proceeds through the intermediacy of **2·BH$_2$Cl** and **2·BHCl$_2$**. Chlorinated products are not seen when the oxidation is carried out in buffered CD_3CN-D_2O. Instead, the disappearance of **2·BH$_3$** is accompanied by the growth of **2·H$^+$**, following a 2:1 stoichiometry of ^{t}BuOCl to **2·BH$_3$** (Figure S13). Boric acid was identified as the ultimate B-containing by-product. Only **2·BH$_2$OD** is observed as plausible intermediate, indicating that its direct hydrolysis leads to **2·H$^+$**, or that further oxidation yields species too hydrolytically labile to accumulate (**2·BH(OD)$_2$** or **2·B(OD)$_3$**). These results are consistent with an oxidative hydrolysis mechanism that involves the electrophilic attack of the tetracoordinate NHC borane by HOCl/^{t}BuOCl.[9,11b,12e] This stands in contrast with the borono-Dakin oxidation of arylboronic acids and their esters, which proceeds through the nucleophilic attack of OCl$^-$ (or HO_2^-, ONOO$^-$) on the Lewis acidic tricoordinate boron center. NMR kinetics experiments carried out with **2·BH$_3$** and ^{t}BuOOH or H_2O_2 reveal kinetic selectivities for hypochlorites over peroxides as high as 10^8 : 1, resulting from the electrophilic oxidation mechanism of NHC boranes (Figures S20-S26).

The bio-imaging capability of **1·BH$_3$** using TPM was then investigated. For the *in situ* detection of ROS, TPM is an attractive method because it uses lower energy light (>700 nm) as the excitation source, limiting photodamage, cellular autofluorescence, and artificial ROS generation.[17] In addition, ratiometric imaging using dual detection windows can rule out experimental artifacts, such as a heterogeneous distribution of the probe, and instrumental variability. After incubation of **1·BH$_3$** for 30 min in live HeLa cells, TPM images were collected with various excitation sources (690-740 nm). Images obtained from excitation at 710 nm were the brightest (Figure S27). They displayed bright emission throughout the cell, except in the nucleus region.

After NaOCl treatment of the cells, spectral changes that parallel those seen in solution occur, allowing for ratiometric image analysis (F_{green}/F_{blue}) with 380–420 nm (F_{blue}) and 480–600 nm (F_{green}). Clearer images were obtained using this ratio (F_{green}/F_{blue}) than with its inverse (F_{blue}/F_{green}); therefore the former was chosen for the analyses.

10.1002/anie.201711188

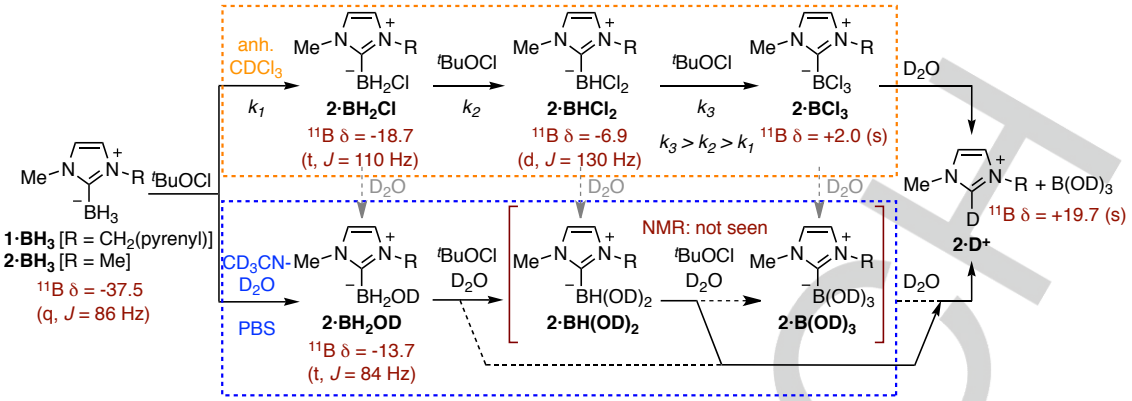

Scheme 1. Mechanistic insight from the NMR titration of **2·BH$_3$** with ^{t}BuOCl as surrogates for **1·BH$_3$** and HOCl, respectively. Plain arrows represent the reaction pathway most consistent with the observed stoichiometry, and dashed arrows alternate plausible pathways.

The average emission ratios (F_{green}/F_{blue}) of **1·BH$_3$** labeled HeLa cells gradually change with NaOCl treatment in a dose-dependent manner (Figure S28). Standard MTT assay indicates that **1·BH$_3$** has no marked cytotoxicity to cells at the low micromolar concentrations used in TPM imaging experiments (Figure S29). The probe is highly photostable under the imaging conditions (Figure S30). Moreover, the values of the F_{green}/F_{blue} ratios for **1·BH$_3$** labeled cells remained nearly constant for 2 h, which is likely due to the fast response of the probe to HOCl in living cells (Figure S31). These outcomes indicated that **1·BH$_3$** is able to detect HOCl in live cells using ratiometric TPM imaging, with minimal interference of cytotoxicity and photobleaching.

A second TPM imaging study was carried out with RAW 264.7 macrophages activated by incubation with lipopolysaccharides (LPS), and then by interferon gamma (IFN-γ). Phorbol myristate acetate (PMA) was used to produce H_2O_2, which is then transformed to HOCl/OCl$^-$ by myeloperoxidase (MPO). When the cells were pretreated with NaOCl, the average emission ratios (F_{green}/F_{blue}) were reduced from 5.13 to 2.50. (Figure 3a and b). Similar results were obtained in the TPM analysis after addition of the stimulants (100 ng mL^{-1} LPS, 50 ng mL^{-1} IFN-γ) followed by 10 nM PMA (Figure 3c). Furthermore, the decrease of average emission ratios (F_{green}/F_{blue}) was moderated when the MPO inhibitors 4-aminobenzoic acid hydrazide (4-ABAH) and flufenamic acid (FAA) were present (Figure 3d and e). These results show that TPM images of **1·BH$_3$** directly reflect the presence of HOCl, as expected from solution assays.

Finally, an investigation was conducted to evaluate the usefulness of **1·BH$_3$** in monitoring HOCl in a fresh rat hippocampal slice. The average emission ratios (F_{green}/F_{blue}) of a slice that had been incubated with **1·BH$_3$** (100 μM) for 1.5 h were 1.57 and 1.63 in the CA1 and CA3 regions, respectively (Figure 4a and b). When tissue slices were pretreated with PMA (10 ng mL^{-1}), the average emission ratios (F_{green}/F_{blue}) dropped to 1.12 and 1.23 in the CA1 and CA3 regions, respectively (Figure 4d and e).

This work demonstrates the potential of B–H bond oxidation-based approaches, in particular those of NHC boranes, in the design of materials that respond to oxidative stress and reactive oxygen species. Oxidative hydrolysis of **1·BH$_3$** occurs selectively for HOCl over other ROS, through an electrophilic mechanism that is distinct from the nucleophilic mechanism for the oxidation of aryl C–B bonds by ROS. The probe **1·BH$_3$** features a ca. 100 nm blue-shift in emission that occur within seconds, is cell permeable, and shows low cytotoxicity. These advantageous properties made **1·BH$_3$** suitable for the ratiometric visualization by TPM of both exogenous and endogenous HOCl, in living cells and tissues. Forthcoming extensions of this design to fluorescent reporters that are less sensitive to aggregation effects than pyrene excimer formation will be required to improve sensitivity in extended assays, Moreover, foreseeable applications of this B–H bond oxidation trigger extend beyond luminescent probes, and to other families of ROS-responsive materials that so far relied on arylboronic acid or ester C–B bond oxidation.

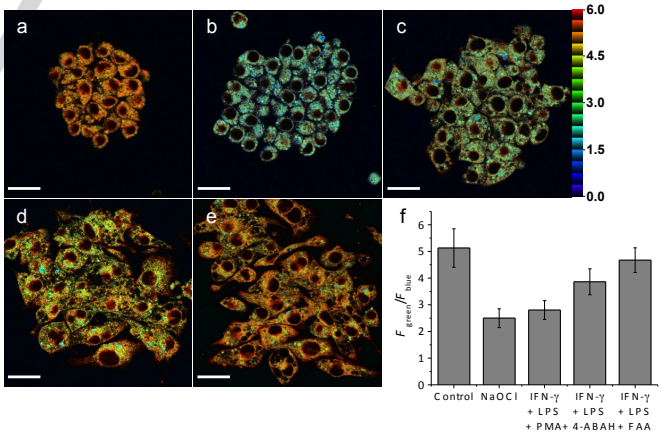

Figure 3. Pseudocolored ratiometric TPM images of RAW 264.7 cells incubated with **1·BH$_3$** (5 μM). (a) Control image. (b) Cells pretreated with NaOCl (200 μM) for 30 min and then incubated with **1·BH$_3$**. (c) Cells pretreated with LPS (100 ng mL-1) for 16 h, IFN- γ (50 ng mL-1) for 4h, PMA (10 nM) for 30 min and then incubated with **1·BH$_3$** for 30 min. (d) Cells pretreated with LPS for 16 h, IFN-γ for 4h, PMA (10 nM) + 4-ABAH (50 μM) for 4h and then **1·BH$_3$** for 30 min. (e) Cells pretreated with LPS for 16 h, IFN-γ for 4h, PMA (10 nM) + FFA (50 μM) for 4h and then **1·BH$_3$** for 30 min. (f) Average F_{green}/F_{blue} intensity ratios in the TPM images. Images were acquired using 710 nm excitation and emission windows of 380–420 nm (blue) and 480–600 nm (green). Scale bars = 20 μm.

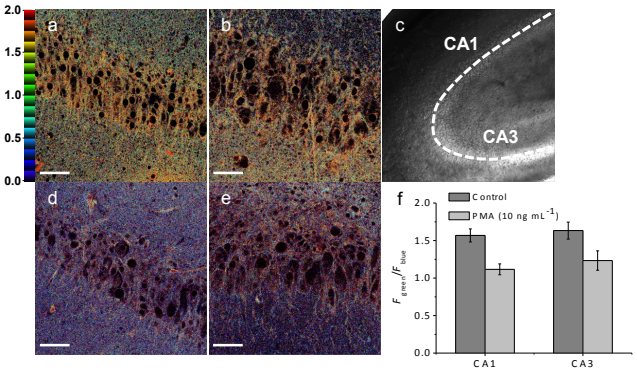

Figure 4. Pseudocolored ratiometric TPM images of a rat hippocampal slice stained with **1·BH$_3$** (100 μM). TPM images of a rat hippocampal slice stained with (a, b) **1·BH$_3$** for 1.5 h and (d, e) pretreated with PMA (10 ng mL^{-1}) for 30 min before labeling with **1·BH$_3$**. TPM images were taken at 40x magnification in the neuron layer of the (a, d) CA1 and (b, e) CA3 regions. (c) Bright-field image of the CA1 and CA3 regions at 10x magnification. (f) Average F_{green}/F_{blue} intensity ratios in the TPM images. Images were acquired using 710 nm excitation and emission windows of 380–420 nm (blue) and 480–600 nm (green). Scale bars = 50 μm.

Acknowledgements

This work was supported by the National Research Foundation of Korea (2012R1A3A2048814 to J. Y.; 2016R1E1A1A02920873 to H. M. K.; and 2015R1D1A1A01059383 to J. B.). We thank Dr. Sung Hong Kim of the Korean Basic Science Institute (Daegu) for EI-MS, and Dr. Su Jin Kim of the Korean Basic Science Institute (Seoul) for ESI-MS analyses.

Keywords: boron • N-heterocyclic carbenes • reactive oxygen species • fluorescence probes • two-photon microscopy

[1] a) L.-C. Lo, C.-Y. Chu, *Chem. Commun.* **2003**, 2728–2729; b) M. Chang, A. Pralle, E. Y. Isacoff, C. J. Chang, *J. Am. Chem. Soc.* **2004**, *126*, 15392–15393; c) E. W. Miller, A. E. Albers, A. Pralle, E. Y. Isacoff, C. J. Chang, *J. Am. Chem. Soc.* **2005**, *127*, 16652–16659; d) L. Du, M. Li, S. Zheng, B. Wang, *Tetrahedron Lett.* **2008**, *49*, 3045–3048; e) N. Karton-Lifshin, E. Segal, L. Omer, M. Portnoy, R. Satchi-Fainaro, D. Shabat, *J. Am. Chem. Soc.* **2011**, *133*, 10960–10965; f) R. Michalski, J. Zielonka, E. Gapys, A. Marcinek, J. Joseph, B. Kalyanaraman, *J. Biol. Chem.* **2014**, *289*, 22536–22553; g) R. D. Hanna, Y. Naro, A. Dieters, P. E. Floreancig, *J. Am. Chem. Soc.* **2016**, *138*, 13353–13360.

[2] a) Q. Xu, K.-A. Lee, S. Lee, K. M. Lee, W.-J. Lee, J. Yoon, *J. Am. Chem. Soc.* **2013**, *135*, 9944–9949; b) Q. Wang, C. Liu, J. Chang, Y. Lu, S. He, L. Zhao, X. Zeng, *Dyes and Pig.* **2013**, *99*, 733–739.

[3] a) A. Sikora, J. Zielonka, M. Lopez, J. Joseph, B. Kalyanaraman, *Free Rad. Biol. Med.* **2009**, *47*, 1401–1407; b) J. Zielonka, A. Sikora, J. Joseph, B. Kalyanaraman, *J. Biol. Chem.* **2010**, *285*, 14210–14216; c) F. Yu, P. Song, P. Li, B. Wang, K. Han, *Analyst* **2012**, *137*, 3740–3749; d) Z. Sun, Q. Xu, G. Kim, S. E. Flower, J. P. Lowe, J. Yoon, J. S. Fossey, X. Qian, S. D. Bull, T. D. James, *Chem. Sci.* **2014**, *5*, 3368–3373.

[4] For recent reviews and accounts, see: a) X. Chen, F. Wang, J. Y. Hyun, T. Wie, J. Qiang, X. Ren, I. Shin, J. Yoon, *Chem. Soc. Rev.* **2016**, *45*, 2976–3016; b) C. Tapeinos, A. Pandit, *Adv. Mater.* **2016**, *28*, 5553–5585; c) T. D. Ashton, K. A. Joliffe, F. M. Pfeffer, *Chem. Soc. Rev.* **2015**, *44*, 4547–4595; d) K. Debowska, D. Debski, M. Hardy, M. Jakubowska, B. Kalyanaraman, A. Marcinek, R. Michalski, B. Michalowski, O. Ouari, A. Sikora, R. Smulik, J. Zielonka, *Pharmacol. Rep.* **2015**, *67*, 756–764; e) J. Zielonka, A. Sikora, M. Hardy, J. Joseph, B. P. Dranka, B. Kalyanaraman, *Chem. Res. Toxicol.*, **2012**, *25*, 1793–1799; f) J. Chan, S. C. Dodani, C. J. Chang, *Nat. Chem.*, **2012**, *4*, 973–984; g) A. R. Lippert, G. C. Van de Bittner, C. J. Chang, *Acc. Chem. Res.*, **2011**, *44*, 793–804.

[5] Some of these claims have been contentious. For discussions, see: a) P. Wardman, *Free Rad. Biol. Med.* **2007**, *43*, 995–1022; b) B. Kalyanaraman, V. Darley-Usmar, K. J. A. Davies, P. A. Dennery, H. J. Forman, M. B. Grisham, G. E. Mann, K. Moore, L. J. Roberts II, H. Ischiropoulos, *Free Rad. Biol. Med.* **2012**, *52*, 1–6; c) V. S. Lin, B. C. Dickinson, C. J. Chang, *Methods Enzymol.* **2013**, *526*, 19–43; d) C. C. Winterbourn, *Biochim. et Biophys. Acta* **2014**, *1840*, 730–738; e) J. Zielonka, R. Podsiadly, M. Zielonka, M. Hardy, B. Kalyanaraman, *Free Rad. Biol. Med.*, **2016**, *99*, 32–42; f) E. J. New, *ACS Sensors* **2016**, *1*, 328–333.

[6] For reviews, see: a) M. E. Roth, O. Green, S. Gnaim, D. Shabat, *Chem. Rev.* **2015**, *116*, 1309–1352; b) A. Alouane, R. Labruère, T. Le Saux, F. Schmidt, L. Jullien, *Angew. Chem. Int. Ed.* **2015**, *54*, 7492–7509; *Angew. Chem.* **2015**, *127*, 7600–7619; c) S. Joshi-Barr, C. de Garcia Lux, E. Mahmoud, A. Almutairi, *Antioxid. Redox Signal.* **2014**, *21*, 730–754; d) G. I. Peterson, M. B. Larsen, A. J. Boydson, *Macromolecules*, **2012**, *45*, 7317–7328.

[7] A. Staubitz, A. P. M. Robertson, M. E. Sloan, I. Manners, *Chem. Rev.* **2010**, *110*, 4023–4078.

[8] For a review: D. P. Curran, A. Solovyev, M. Makhlouf Brahmi , L. Fensterbank, M. Malacria, E. Lacôte, *Angew. Chem. Int. Ed.* **2011**, *50*, 10294–10317; *Angew. Chem.* **2011**, *123*, 10476–10500.

[9] A. Solovyev, Q. Chu, S. J. Geib, L. Fensterbank, M. Malacria, E. Lacôte, D. P. Curran, *J. Am. Chem. Soc.* **2010**, *132*, 15072–15080.

[10] S. Gardner, T. Kawamoto, D. P. Curran, *J. Org. Chem.* **2015**, *80*, 9794–9797.

[11] a) S.-H. Ueng, M. Makhlouf Brahmi, É. Derat, L. Fensterbank, E. Lacôte, M. Malacria, D. P. Curran, *J. Am. Chem. Soc.* **2008**, *130*, 10082–10083; b) S.-H. Ueng, L. Fensterbank, M. Malacria, D. P. Curran, *Org. Biomol. Chem.* **2011**, *9*, 3415–3420.

[12] a) Q. Chu, M. Makhlouf Brahmi, A. Solovyev, S.-H. Ueng, D. P. Curran, M. Malacria, L. Fensterbank, E. Lacôte, *Chem. Eur. J.* **2009**, *15*, 12937–12940; b) D. M. Lindsay, D. McArthur, *Chem. Commun.* **2010**, *46*, 2474–2476; c) M. Horn, H. Mayr, E. Lacôte, E. Merling, J. Deaner, S. Wells, T. McFadden, D. P. Curran, *Org. Lett.* **2012**, *14*, 82–85; d) T. Taniguchi, D. P. Curran, *Org. Lett.* **2012**, *14*, 4540–4543; e) V. Lamm, X. Pan, T. Taniguchi, D. P. Curran, *Beilstein J. Org. Chem.* **2013**, *9*, 675–680.

[13] a) T. Förster, *Angew. Chem.* **1969**, *81*, 364; *Angew. Chem. Int. Ed.* **1969**, *8*, 333; b) F. M. Winnik, *Chem. Rev.* **1993**, *93*, 587. c) S. Karuppannan, J.-C. Chambron, *Chem. Asian J.* **2011**, *6*, 964; d) E. Manandhar, K. J. Wallace, *Inorg. Chim. Acta* **2012**, *381*, 15.

[14] For recent examples of fluorescent probes for ROS that rely on the pyrene excimer, see ref. 3c, and: a) C.-C Zhang, Y. Gong, Y. Yuan, A. Luo, W. Zhang, J. Zhang, X. Zhang, W. Tan, *Anal. Methods* **2014**, *6*, 609–614; b) Y. Wu, J. Wang, F. Zeng, S. Huang, J. Huang, H. Xie, C. Yu, S. Wu, *ACS Appl. Mater. Interfaces*, **2016**, *8*, 1511–1519.

[15] a) H. M. Kim, B. R. Cho, *Chem. Rev.* **2015**, *115*, 5014-5055; b) S. W. Perry, R. M. Burke, E. B. Brown, *Ann. Biomed. Eng.* **2012**, *40*, 277-291; c) F. Helmchen, W. Denk, *Nat. Methods.* **2005**, *2*, 932-940.

[16] a) C. C. King, M. M. Jefferson, E. L. Thomas, *J. Leukoc. Biol.* **1997**, *61*, 293–302; b) C. C. Winterbourn, M. B. Hampton, J. H. Livesey, A. J. Kettle, *J. Biol. Chem.* **2006**, *281*, 39860–39869; c) Y. W. Yap, M. Whiteman, N. S. Cheung, *Cell. Signal.* **2007**, *19*, 219–228.

[17] M.-J. Jou, S.-B. Jou, M.-J Guo, H.-Y. Wu, T.-I. Peng, *Ann. N. Y. Acad. Sci.*, **2004**, *1011*, 45–56.

10.1002/anie.201711188

WILEY-VCH

COMMUNICATION

Bleached Boranes: NHC boranes are oxidatively hydrolyzed to imidazolium salts with high kinetic selectivity for HOCl over other reactive oxygen species. This reactivity is harnessed in the two-photon fluoresence imaging probe **1·BH$_3$**, the first ROS-responsive material that rely on a B–H bond oxidation as triggering event.

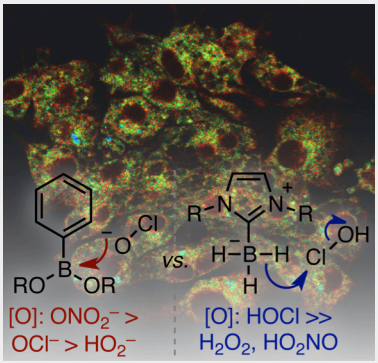

Yen Leng Pak,[†] Sang Jun Park,[†] Di Wu,[†] BoHyun Cheon, Hwan Myung Kim, Jean Bouffard,* and Juyoung Yoon**

Page No. – Page No.

N-Heterocyclic Carbene Boranes as Reactive Oxygen Species-Responsive Materials: Application to the Two-Photon Imaging of Hypochlorous Acid in Living Cells and Tissues